Precambrian Research 259 (2015) 130–142

Contents lists available at ScienceDirect

Precambrian Research

journal homepage: www.elsevier.com/locate/precamres

New paleomagnetic results from the Ediacaran Doushantuo Formation in South China and their paleogeographic implications

Shihong Zhang[a,*], Haiyan Li[a], Ganqing Jiang[b], David A.D. Evans[c], Jin Dong[a,d], Huaichun Wu[a], Tianshui Yang[a], Pengju Liu[d], Qisheng Xiao[a]

[a] State Key Laboratory of Biogeology and Environmental Geology, China University of Geosciences, Beijing 100083, China
[b] Department of Geoscience, University of Nevada, Las Vegas, NV 89154-4010, USA
[c] Department of Geology and Geophysics, Yale University, New Haven, CT 06520-8109, USA
[d] Institute of Geology, Chinese Academy of Geological Sciences, Beijing 100037, China

ARTICLE INFO

Article history:
Received 28 May 2014
Received in revised form
15 September 2014
Accepted 19 September 2014
Available online 28 September 2014

Keywords:
Paleomagnetism
Doushantuo Formation
South China
Ediacaran
Supercontinent reconstruction

ABSTRACT

A new paleomagnetic pole is obtained from the top of Member 3 of the Doushantuo Formation in the Jiulongwan section of the Yangtze Gorges area in South China. A total of 191 samples from 23 sites were collected and subjected to stepwise alternating field (AF) and thermal demagnetization. After the removal of a soft component (SC) of viscous magnetic remanence acquired in present geomagnetic field, a high temperature component (HC), likely carried by magnetite, was isolated. The HC includes vectors from 147 samples using principal component analysis and arc constraints from 44 samples using remagnetization great-circle analysis. Both the vectors only and the combined vectors and arc constraints of the HC passed a reversal test. This is the first Ediacaran paleomagnetic remanence from the South China Block (SCB) that passes a reversal test, and it is interpreted as a primary remanence. The HC vectors were thus used to calculate the paleomagnetic pole, and in combination with arc constraints, were used for polarity interpretation. The vectors give a mean direction of ($D = 75.2^\circ$, $I = 41.0^\circ$, $\alpha_{95} = 2.5^\circ$, $N = 147$) after bedding correction, and a corresponding paleomagnetic pole at 23.9° N, 187.0° E (dm/dp = 3.0/1.8). This pole differs significantly from previously published results of the Doushantuo Formation, which may have been subjected to Paleozoic remagnetization. Our results provide a $23.5 \pm 1.8^\circ$ N paleolatitude for the Yangtze Gorges area of the SCB and suggest several alternative paleogeographic options for the Ediacaran–Cambrian amalgamation of East Gondwana, depending on chronostratigraphic correlations.

1. Introduction

The South China Block (SCB) is one of the most intensively investigated Neoproterozoic tectonic units for its well-preserved records encompassing some of the major geological, biological and geochemical events including the breakup of supercontinent Rodinia and assembly of Gondwana, the initiation and meltdown of the most severe glaciations in Earth history, the rise of early animal life and possible ocean oxygenation events. A reliable paleogeographic reconstruction for the SCB is crucial for understanding the potential causal links between these geological, biological and geochemical events. Existing paleogeographic reconstructions pose uncertainties or controversies on whether, when and how the SCB was connected to Australia and India, and the position of the SCB during the 'snowball' Earth times (e.g., Jiang et al., 2003; Macouin et al., 2004; Hoffman and Li, 2009; Li et al., 2013, 2014; Zhang et al., 2013; Yao et al., 2014).

In some paleogeographic reconstructions, the SCB was placed close to the paleo-equator through the Ediacaran Period (ca. 635–541 Ma). Evidence supporting this low-latitude position was from an eastward, shallow remanent magnetization observed from the Doushantuo Formation (ca. 635–551 Ma) in the Yangjiaping Section, northern Hunan Province (Macouin et al., 2004; Fig. 1a). However, the primary origin of this paleomagnetic direction has been questioned (Zhang et al., 2013) because, (1) it does not contain the pattern of numerous Ediacaran geomagnetic field reversals observed in Australia (e.g., Sohl et al., 1999; Raub, 2008; Schmidt et al., 2009; Schmidt and Williams, 2010); (2) the calculated paleomagnetic pole is similar to Early Cambrian and Silurian poles of the SCB; and (3) the positive fold test only constrains the magnetization to pre-Jurassic in age. Therefore, a more rigorous examination is required.

* Corresponding author. Tel.: +86 10 82322257; fax: +86 10 82321983.
E-mail address: shzhang@cugb.edu.cn (S. Zhang).

http://dx.doi.org/10.1016/j.precamres.2014.09.018
0301-9268/

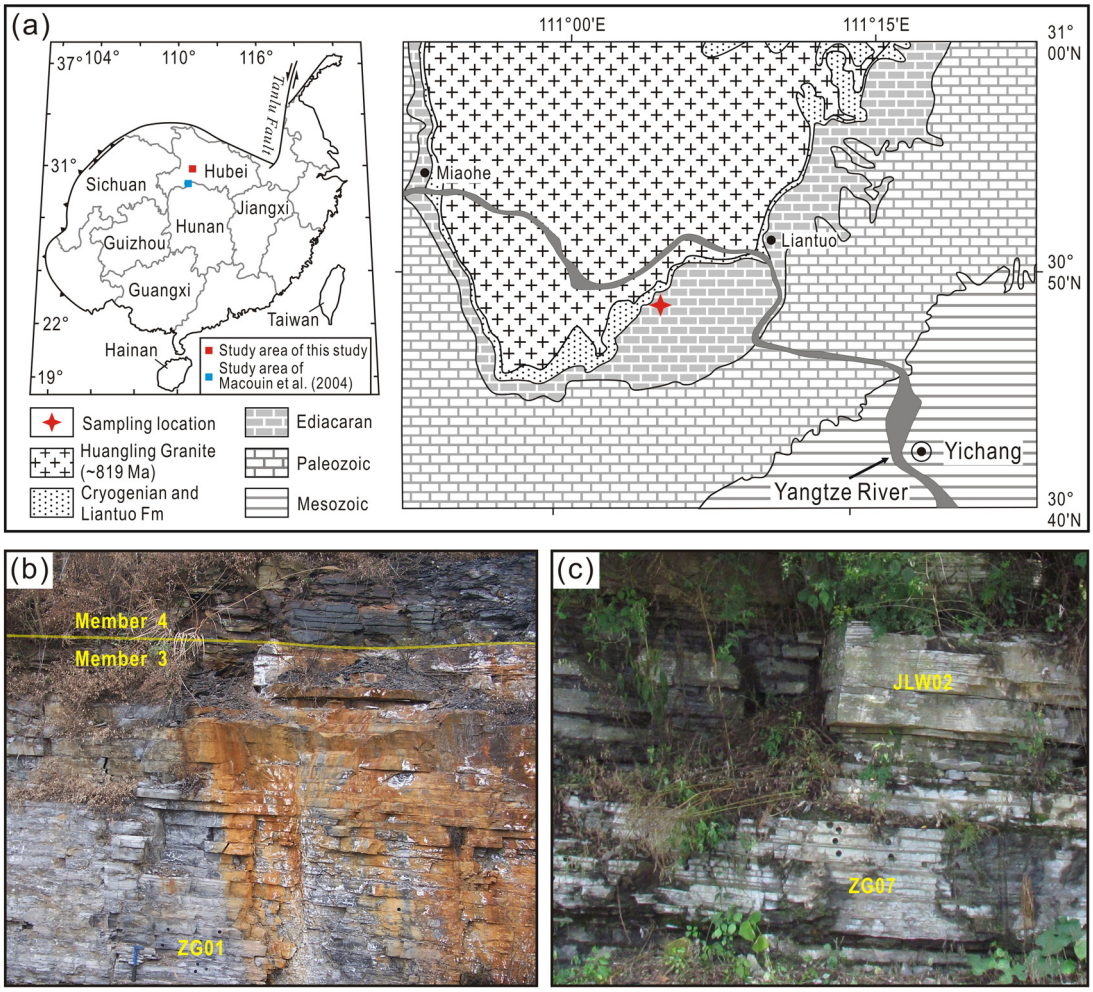

Fig. 1. (a) Simplified Geological map of the Yangtze Gorge region showing the sampling location. (b) and (c) Typical outcrop photos of the dolomite/limestone ribbon rocks of the upper Member 3 of the Doushantuo Formation, with paleomagnetic sites labeled. The diameter of paleomagnetic drilling holes is ~2.5 cm.

In this paper, we report new paleomagnetic results that pass a reversal test from the upper Doushantuo Formation in the Yangtze Gorges area of the SCB. The new data are significantly steeper than those previously determined (e.g., Macouin et al., 2004), fill the gap of the paleomagnetic database of the SCB between ca. 635 Ma and Early Cambrian, and provide important constraints for the Ediacaran paleogeographic position of the SCB.

2. Geological background and sampling

The SCB contains the Yangtze Block (YB) in the northwest and the Cathaysia Block in the southeast. Almost all the available Precambrian paleomagnetic data for the SCB are from the YB, because the Precambrian strata in the Cathaysia Block are poorly dated and strongly deformed. Although no paleomagnetic data are available from the Cathaysia Block, paleogeographic reconstructions commonly place the Cathaysia and Yangtze Blocks as one coherent continental unit since ca. 900 Ma (e.g., Li et al., 2008).

Neoproterozoic strata in the YB are well dated and consist of three major parts (Fig. 2): (1) the pre-Cryogenian siliciclastic units in the lower part, represented by the Liantuo Formation/Banxi Group, with ages ranging from ~820 Ma to ~720 Ma (Zhang et al., 2008a,b); (2) the Cryogenian glacial and interglacial deposits in the middle, including two glacial diamictite intervals (the Chang'an/Dongshanfeng formations and the Nantuo Formation) separated by interglacial manganese-bearing shale/siltstone of the Datangpo/Xiangmeng formations dated between ~663 and ~654 Ma (Zhou et al., 2004; Zhang et al., 2008a,c); and (3) the Ediacaran mixed carbonate-siliciclastic units assigned to the Doushantuo and Dengying/Liuchapo formations at the top.

The Doushantuo Formation was deposited along a passive margin, facing southeast in present-day coordinates (Jiang et al., 2011). In the Yangtze Gorges area, the Doushantuo Formation conformably overlies the Nantuo glacial diamictite and is divided into four members (Fig. 2). Member 1 refers to the ca. 5-m-thick cap carbonate at the base of the Doushantuo Formation. Member 2 consists of ~100-m-thick alternating organic-rich shale and carbonates with abundant pea-sized chert nodules. Member 3 consists of 60–80-m-thick limestone and dolostone with thin shaly interbeds. Member 4 refers to the ca. 10-m-thick black, organic-rich shale interval at the top of the Doushantuo Formation, containing abundant carbonate concretions (Dong et al., 2013). The cap carbonate of Member 1 and the organic-rich black shale of Member 4 are the stratigraphic marker beds for regional correlations of the Doushantuo Formation (Jiang et al., 2011). A prominent negative $\delta^{13}C$ excursion from Members 3 and 4 was intensively studied in many exposed sections of the YB, and has been correlated with the Shuram $\delta^{13}C$ excursion in Oman and Wonoka $\delta^{13}C$ anomaly in Australia (e.g., Jiang et al., 2007; Zhou and Xiao, 2007; Zhu et al., 2007, 2013b; Sawaki et al., 2010; Tahata et al., 2013).

The age of the Doushantuo Formation in the Yangtze Gorges area is constrained by a few zircon U–Pb ages (Condon et al., 2005;

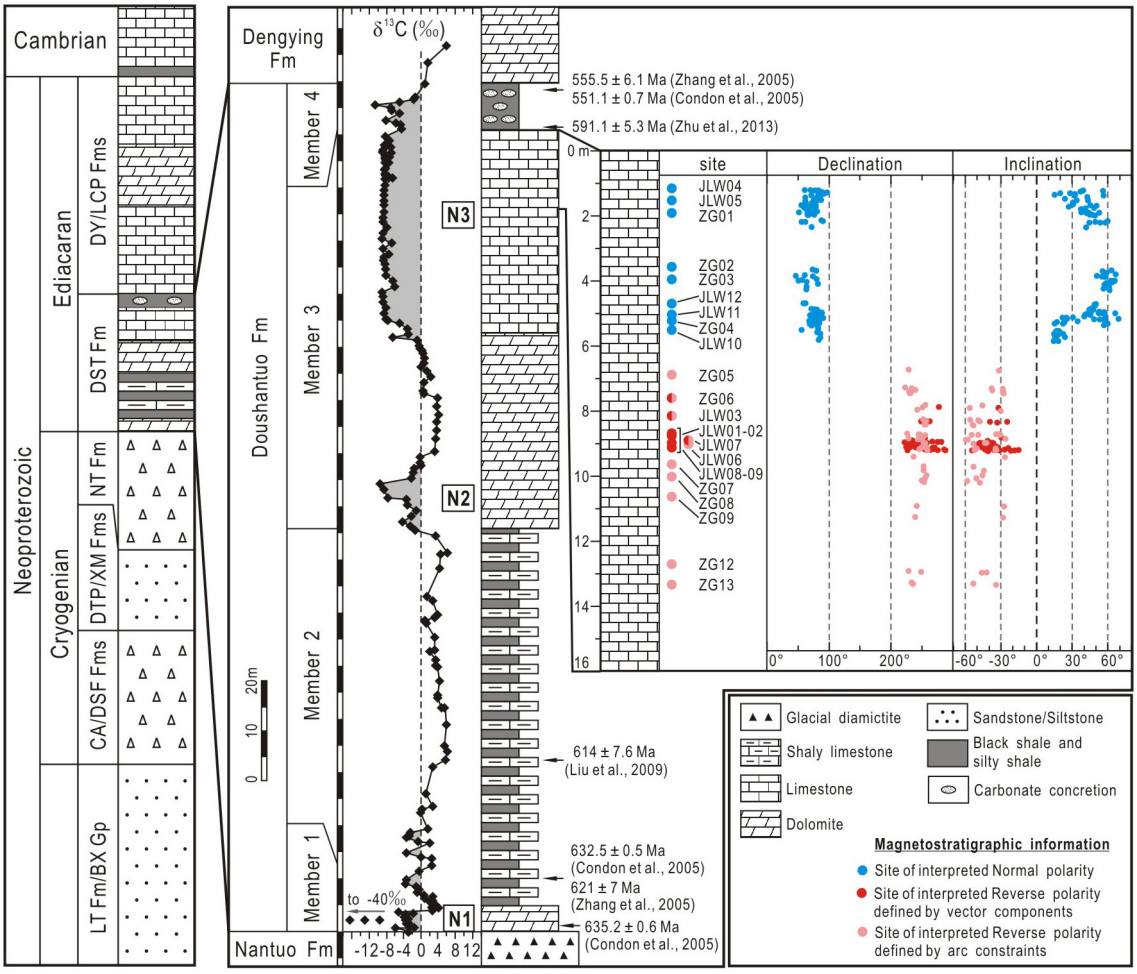

Fig. 2. Stratigraphic variation of the high temperature component (HC) in the Member 3 of the Doushantuo Formation from the Jiulongwan section, showing declinations and inclinations in tilt-corrected coordinates. Stratigraphic columns and carbon isotopic data are after Jiang et al. (2007). Fm, Formation; Gp, Group; LT, Liantuo Formation; BX, Banxi Group; CA, Chang'an Formation; DSF, Dongshanfeng Formation; DTP, Datangpo Formation; XM, Xiangmeng Formation; NT, Nantuo Formation; DST, Doushantuo Formation; DY, Dengying Formation; LCP, Liuchapo Formation.

Zhang et al., 2005; Fig. 1b). The ash beds within the Doushantuo cap carbonate (Member 1), at the base of Member 2, and at the top of Member 4 were dated at 635 ± 0.6 Ma, 632 ± 0.5 Ma, and 551 ± 0.7 Ma, respectively (Condon et al., 2005). A U–Pb SHRIMP age of 614 ± 7.6 Ma was also reported from a tuffaceous bed in the middle Member 2 of the Zhangchunping section (Liu et al., 2009), but the distribution of this ash bed is limited and its correlation with other sections is uncertain. Recently, Zhu et al. (2013a) reported a Re–Os age of 591 ± 5.3 Ma for the black shales at the bottom of Member 4, but this age was determined after excluding the discordant data points.

Our new paleomagnetic study was conducted in the Jiulongwan section, ~20 km west of the Yichang city (30°48.6′N, 111°4.4′E), Hubei province (Fig. 1). Paleomagnetic sampling covers the uppermost 14 m of Member 3 (Fig. 2). The sampled interval is composed of thinly laminated limestone-dolomite "ribbon" rocks (Fig. 1b and c) that have negative $\delta^{13}C$ values of −6‰ to −8‰, covering the upper part of the $\delta^{13}C$ excursion ("N3" in Jiang et al., 2007).

A total of 191 samples were collected from 23 stratigraphic sites using a gasoline-powered drill (Fig. 2). Among these samples, 59 samples were collected from 11 sites (ZG01-09, ZG12-13) in 2007, and 132 samples were collected from 12 sites (JLW01-12) in 2013. Samples were oriented using a magnetic compass and a sun compass when possible. No significant difference was observed between results using the two devices.

3. Paleomagnetic experiments and results

3.1. Laboratory conditions and procedures

Samples of ZG01-09 and ZG12-13 were subjected to stepwise alternating field (AF) and thermal demagnetization in the paleomagnetic laboratory of Yale University; while samples of JLW01-12 were subjected to thermal demagnetization in Paleomagnetism and Environmental Magnetism Laboratory in China University of Geosciences, Beijing (CUGB). Samples and instruments in both laboratories were kept in a μ-metal shielded room during the demagnetization process, with ambient magnetic fields typically 100–300 nT in the sample loading, transfer, and storage regions, and <10 nT in the magnetometer measurement and furnace heating/cooling zones.

For ZG01-09 and ZG12-13 samples, which were trimmed to 0.7 cm-high right cylinders, remanent magnetizations were measured using a 2G superconducting magnetometer outfitted with automated sample changing capabilities (Kirschvink et al., 2008), and thermal demagnetization was carried out using a TD-48 thermal demagnetizer (ASC Scientific) in a N_2 atmosphere. AF demagnetization was carried out using a Molspin tumbling demagnetizer. After natural remanent magnetization (NRM) measurements, low-field AF demagnetization (reaching peak alternating field of 15 mT in 2.5 mT steps) was applied. Then

the samples were cooled and re-warmed in a shielded liquid N_2 basin through the Morin transition of hematite (258 K) and the Verwey transition of magnetite (120 K). These treatments were considered to have removed viscous remanence carried by multi-domain particles of hematite or magnetite (Özdemir et al., 2002). After this procedure, the specimens were subjected to further step-wise thermal demagnetization at 170, 185, 200, 220, 240, 260, 280, 290, 300, 310, 320, 325, 335, 345, 360, 380, 400, 420, 435, 447, 456, 466, 470 °C. All 59 samples were demagnetized through these steps until their directional behavior became unstable due to acquisition of spurious magnetizations.

For JLW01-12 samples, which were trimmed to 2.2 cm-high right cylinders, remanent magnetizations were measured using a 2G 755-4K superconducting magnetometer, and thermal demagnetization was carried out using a TD-48 thermal demagnetizer in air. After NRM measurements, all 132 specimens were subjected to step-wise thermal demagnetization at 100, 150, 170, 200, 240, 280, 300, 315, 330, 360, 390, 410, 430, 450, 470, 500 °C, until the remanence directions became unstable.

3.2. Paleomagnetic results

No systemic difference is observed between the paleomagnetic experiments from the two laboratories in Yale and CUGB. The NRM intensities of the samples are of 1–10 mA/m. Based on the stability of remanence, we divided the samples into two groups. Group 1 data, with 147 samples, are characterized by both a soft component (SC) and a hard component (HC), each of which can be identified as a linear vector using principal component analysis (PCA) (Kirschvink, 1980; Fig. 3a–f). Group 2 data, with 44 samples, have a SC that can be calculated as a linear vector using PCA, but the HC can only be inferred by remagnetization great circles on stereographic plots (Fig. 3g and h).

For group 1 samples, the SC was determined mostly below 200 °C or by low alternating field. Directions of this component (in situ) are close to the present geomagnetic field in this region (D = 356.6°, I = 47.2°, IGRF, online data). The SC from these samples is thus interpreted as a component from recent, viscous remanent magnetization (VRM) (Fig. 4). Mean direction of the SC is D_g = 1.2°, I_g = 43.4°, α_{95} = 1.15° in the geographic coordinates, and D_s = 7.9°, I_s = 43.4°, α_{95} = 1.17° after tilt correction. The HC was defined generally between 315 °C and 490 °C. The unblocking temperature of the HC is near to, but lower than, the Curie temperature of magnetite (~575 °C), suggesting that it is probably carried by detrital, Ti-bearing magnetite. This is supported by the stepwise thermal demagnetization of three orthogonal isothermal remanent magnetization (IRM) directions (after Lowrie, 1990) for representative samples (Fig. 5). The HC has dual-polarity (Figs. 2b and 6a): directed westward and moderately up (spanning the lower 8 m of the sampling section), or eastward and moderately down (spanning the upper 6 m). The HC passed a reversal test of "B" Class (Table 1; McFadden and McElhinny, 1990). The magnetostratigraphic pattern (Fig. 2) may have recorded a geomagnetic field reversal during deposition of the Doushantuo Formation, and is interpreted to be primary in the sense of either a detrital-remanent magnetization (DRM), a post-depositional remanent magnetization (pDRM), an early diagenetic chemical-remanent magnetization (CRM), or some combination thereof. The sample-level average HC direction (of the 147 specimens) is D_g = 72.8°, I_g = 47.6°, α_{95} = 2.5° in geographic coordinates, and D_s = 75.2°, I_s = 41.0°, α_{95} = 2.5° in stratigraphic coordinates (Table 1). On site level (n = 14), the average direction is D_g = 72.0°, I_g = 48.8°, α_{95} = 7.2° in geographic coordinates, and D_s = 74.3°, I_s = 42.2°, α_{95} = 7.4° in stratigraphic coordinates (Table 1).

Interestingly, group 1 remanence vectors from the upper polarity zone show systematic trends in inclination through the strata (Fig. 2). It is not clear whether such trends are due to (i) differing degrees of unresolved SC contamination of the HC remanence, (ii) variable amounts of sedimentary inclination shallowing in the HC remanence, (iii) paleolatitude shifts of the SCB during Doushantuo deposition, or (iv) geomagnetic excursions or enhanced paleosecular variation of the Ediacaran geodynamo. Given that the aggregate HC data pass a Class "B" reversal test, the first explanation (i) seems unlikely. Inclination shallowing (ii) remains an important problem in paleomagnetic studies of sedimentary rocks, but quantification can be impractical (e.g., Schmidt, 2014). We note that the inclination variance of our data is larger than expected from geomagnetic field models (Tauxe and Kent, 2004), so there does not exist a single correction factor that can uniformly explain the Doushantuo inclination variability. Furthermore, hypothesis (ii) implies that some stratigraphic intervals are much more strongly compacted than others, which is not supported by invariant lithofacies characteristics through the measured section. In addition, our paleogeographic reconstructions of the SCB with Australia rely entirely on sedimentary paleomagnetic results with moderate inclinations, which may be shallowed to various degrees, but the large-scale relative paleogeographic motions are dominated by variations in declination instead of inclination. Thus, the shallowing effects are likely to be minor. Hypothesis (iii) would need to be tested by detailed sampling of additional sections of Doushantuo Member 3 or time-equivalent units across the SCB. Hypothesis (iv) cannot be excluded, but such explanations are ad hoc and would need to be verified by detailed, additional study.

For group 2 samples, the PCA-defined SC directions resemble those of group 1. It is thus interpreted as a VRM of the recent geomagnetic field. However, the residual magnetization of the samples became too weak to be measured when they were heated over ~330 °C. In these cases, the HC cannot be fitted directly by high-temperature vectors decaying to the origin. We applied the remagnetization circle analysis for these samples (McFadden and McElhinny, 1988), by combining the arc-constraint components with those vector-fit components of group 1 samples (Fig. 6b). While the vector-fit components of the group 1 samples are sub-equally divided between the two polarities, the arc constraints from group 2 samples mainly appear in the lower polarity zone. The arc constraints extrapolate beyond the ends of long remagnetization circles, which is consistent with the hypothesis that arc constraints primarily reflect incompletely removed VRM (Haggart et al., 2009; Zhang et al., 2013).

The HC, combining both vectors and arc constraints, also passed a reversal test of "B" Class (Table 1; McFadden and McElhinny, 1990). The sample-level average HC direction (of the 191 samples, and number of the arcs was weighted by 0.5 for averaging in this study, N = 169) is D_g = 71.4°, I_g = 47.8°, α_{95} = 2.3° in geographic coordinates, and D_s = 73.9°, I_s = 41.3°, α_{95} = 2.3° in stratigraphic coordinates (Table 1). The site-level (n = 18) mean direction is D_g = 69.4°, I_g = 49.3°, α_{95} = 5.5° in geographic coordinates, and D_s = 71.7°, I_s = 42.7°, α_{95} = 5.6° after bedding correction. There is no significant difference between the results that included the arc constraints and those that only used the PCA vectors (Table 1). The data from group 2 are all in the lower part of our sampled section (Fig. 2), supporting the interpretation derived from group 1 vector data, in which only one geomagnetic reversal occurred during the deposition of these strata.

Four methods have been used to calculate the corresponding paleomagnetic pole: (i) Based on the sample-level direction average, and using all the usable directions of the HC (groups 1 and 2), the paleomagnetic pole is at 25.1° N, 187.3° E, dm/dp = 2.8°/1.7°; (ii) Averaging the site-level Virtual Geomagnetic poles (VGPs), using all usable observations of groups 1 and 2, the pole is at 26.7° N, 186.2° E, A_{95} = 5.4°; (iii) Based on the sample-level direction average and using the vector-fit data (group 1) only, the paleomagnetic pole is at 23.9° N, 187.0° E, dm/dp = 3.0°/1.8°; and (iv) Averaging

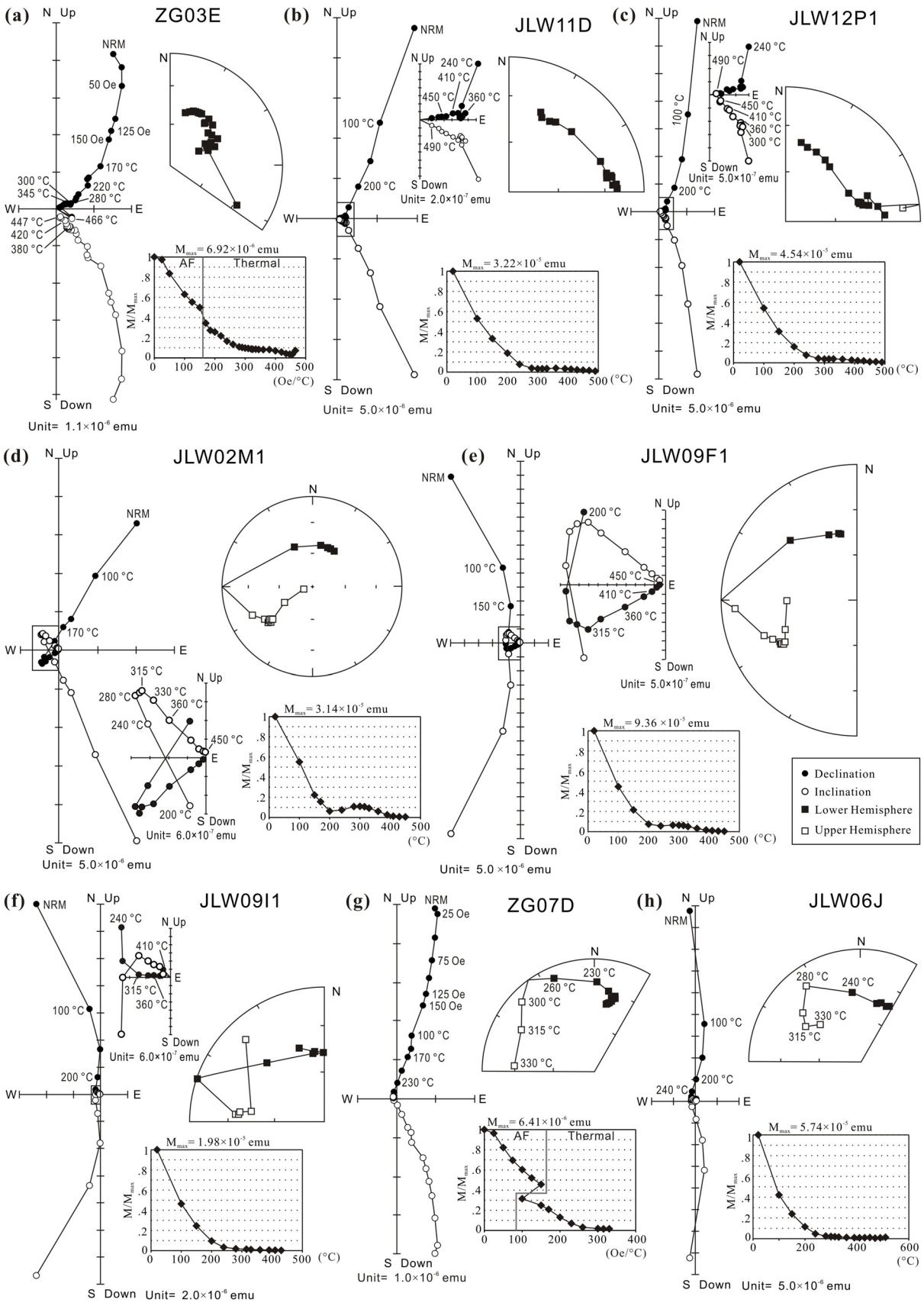

Fig. 3. Typical demagnetization trajectories, in tilt-corrected coordinates. (a)–(c) Typical samples of the polarity 1. (d)–(f) Typical samples of the polarity 2, whose high temperature components (HCs) are identified using principal components analysis (PCA) (Kirschvink, 1980). (g) and (h) Typical samples of polarity 2, whose HCs are defined by arc constraints.

Table 1
Paleomagnetic results for the high-temperature component (HC) of Doushantuo Formation Member 3 in South China, Jiulongwan (30.810° N, 111.073° E).

Site	Total, L C	N/n	In geographic coordinates							In stratigraphic coordinates						dm/dp A_{95} (°)
			D (°)	I (°)	k	α_{95} (°)	Plat (° N)	Plon (° E)	dm/dp A_{95} (°)	D (°)	I (°)	k	α_{95} (°)	Plat (° N)	Plon (° E)	
JLW04	18, 18L0C	18	76.8	40.2	33.9	6.0	22.3	186.9	7.2/4.4	80.4	33.7	34.0	6.0	17.3	189.6	6.8/3.9
JLW05	18, 18L0C	18	63.3	47.2	65.5	4.3	35.8	186.4	5.6/3.6	69.2	41.8	65.1	4.3	29.2	188.9	5.3/3.2
ZG01	6, 6L0C	6	78.6	57.6	40.0	9.8	26.8	170.7	14.4/10.5	75.9	51.9	40.2	9.8	26.9	177.5	13.4/9.1
ZG02	6, 6L0C	6	75.6	64.7	124.3	5.5	31.3	162.2	8.8/7.1	72.6	58.9	124.6	5.5	31.6	170.7	8.2/6.1
ZG03	10, 10L0C	10	64.2	67.0	129.3	4.0	39.2	159.9	6.6/5.5	63.0	61.1	129.8	4.0	39.3	169.6	6.1/4.7
JLW12	15, 15L0C	15	71.2	51.3	128.0	3.4	30.4	179.7	4.6/3.1	75.3	44.2	127.9	3.4	24.8	184.5	4.3/2.7
JLW11	10, 10L0C	10	80.1	30.5	212.5	3.3	16.6	191.6	3.7/2.0	81.5	23.0	210.3	3.3	13.3	194.9	3.5/1.9
ZG04	14, 14L0C	14	82.2	64.1	125.7	3.4	26.7	161.7	5.4/4.3	78.1	58.5	125.7	3.4	27.4	169.8	5.0/3.7
JLW10	13, 13L0C	13	80.2	25.7	100.5	4.2	15.2	194.2	4.5/2.4	81.3	18.2	100.8	4.2	12.2	197.4	4.4/2.3
ZG05-06	11,1L10C	6	236.7	−42.7	30.4	8.4	−40.0	13.3	10.4/6.4	239.3	−35.4	26.5	9.0	−35.8	18.2	10.4/6.0
JLW03	8, 3L5C	5.5	251.9	−51.8	51.2	7.8	−30.0	359.0	10.6/7.3	255.7	−44.4	50.6	7.9	−24.6	4.2	9.9/6.2
JLW01-02	12, 11L1C	11.5	243.6	−44.0	20.2	9.9	−34.5	9.3	12.4/7.8	248.5	−37.3	20.2	9.9	−28.5	12.6	11.6/6.8
JLW07	15, 5L10C	10	248.7	−50.9	27.6	7.4	−32.3	0.9	10.0/6.7	252.3	−44.2	27.8	7.4	−27.3	5.7	9.3/5.8
JLW06	5, 0L5C	2.5	248.6	−47.5	59.8	10.0	−31.4	4.3	13.0/8.4	251.3	−41.0	61.0	9.9	−27.2	8.6	12.0/7.3
JLW08	6, 5L1C	5.5	223.5	−51.6	83.3	7.4	−53.1	7.2	10.1/6.9	230.8	−46.9	90.1	7.1	−46.1	11.2	9.2/5.9
JLW09	11, 11L0C	11	252.7	−39.9	23.1	9.7	−25.7	8.9	11.7/7.0	255.3	−32.8	23.1	9.7	−21.4	12.5	11.0/6.2
ZG07-08	5, 0L5C	2.5	251.4	−56.5	205.6	5.4	−31.8	354.0	7.8/5.6	254.1	−50.3	183.6	5.7	−27.8	359.7	7.6/5.1
ZG09-13	7, 0L7C	3.5	238.5	−46.5	53.3	8.3	−39.5	8.9	10.7/6.9	240.3	−40.1	43.9	9.2	−36.2	14.0	11.1/6.7
Sample-level average for groups 1 and 2, $N = 169$			71.4	47.8	23.6	2.3	29.2	182.9	3.0/2.0	73.9	41.3	22.8	2.3	25.1	187.3	2.8/1.7
Site-level average for groups 1 and 2, $n = 18$			69.4	49.3	40.5	5.5	31.6	181.1	$A_{95} = 5.5$	71.7	42.7	38.5	5.6	26.7	186.2	$A_{95} = 5.4$
Sample-level average for group 1, $N = 147$			72.8	47.6	22.8	2.5	28.0	182.6	3.3/2.1	75.2	41.0	22.2	2.5	23.9	187.0	3.0/1.8
Site-level average for group 1, $n = 14$			72.0	48.8	31.1	7.2	29.5	180.4	$A_{95} = 7.4$	74.3	42.2	29.8	7.4	25.9	185.5	$A_{95} = 6.7$

Total, number of samples demagnetized; L, number of samples with vector component; C, number of samples with arc constraints only; N, number of samples for statistics (vector is weighted by 1, arc weighted by 0.5); n, number of sites for statistics; D, declination; I, inclination; k, Fisher precision parameter of the mean; α_{95}/A_{95}, radius of circle of 95% confidence about the mean direction/pole; Plat/Plon, latitude/longitude of VGP; dm/dp, semi-axes of elliptical error around the pole at a probability of 95%.
Vector components pass a reversal test (McFadden and McElhinny, 1990), class B, with a critical angle 9.2°, angular difference is 4.6°. Components combined with vector and arc constraints also pass a reversal test, class B, with a critical angle 9.2°, angular difference is 4.6°.

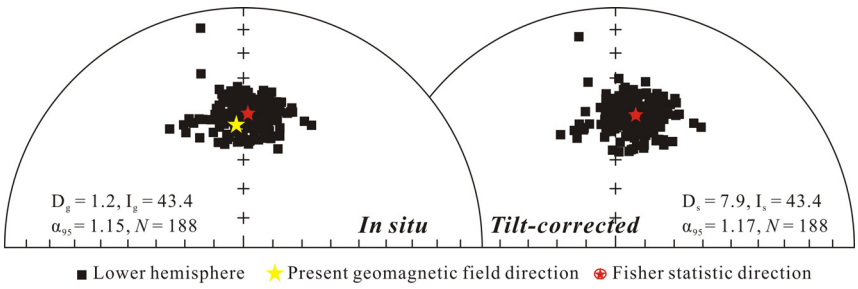

Fig. 4. Equal area projections of the soft component directions.

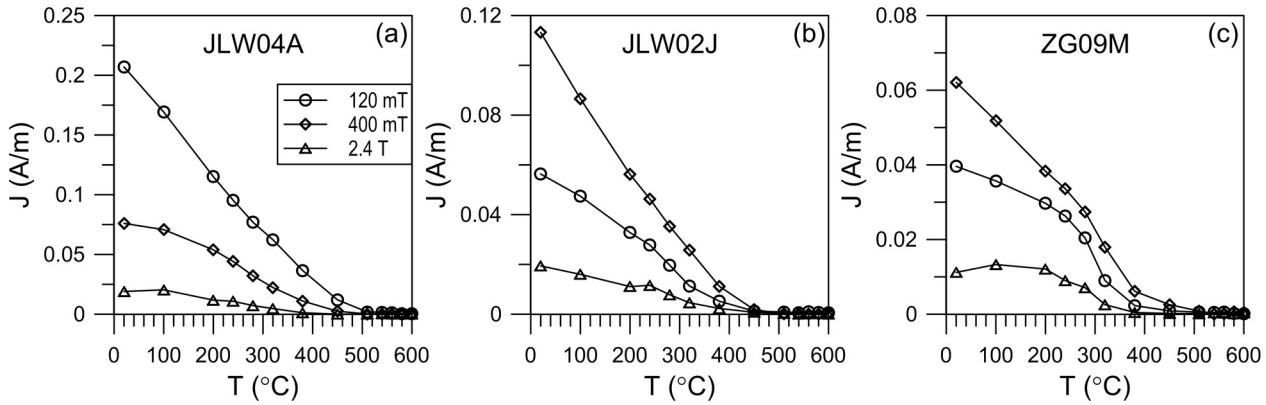

Fig. 5. Stepwise thermal demagnetization of the three orthogonal directions held by isothermal remanent magnetization (IRM) (after Lowrie, 1990) for representative samples of (a) the polarity 1, (b) the polarity 2, whose HC is identified using PCA, and (c) the polarity 2, whose HC is defined by arc constraints.

the site-level VGPs, but using the group 1 data only, the pole is at 25.9° N, 185.5° E, A_{95} = 6.7°. There is no significant difference observed between the results of these methods, but we favor the result of method (iii), i.e., using the vector-fit data only to calculate the pole and paleolatitude. The new paleomagnetic pole does not resemble any younger poles of the SCB (Fig. 7a), adding confidence to its reliability.

3.3. Comparison with previous results

Our new results differ from the previously reported paleomagnetic pole and inclination (0.6° N, 196.9° E, dp/dm = 4.5°/9°) from the Doushantuo Formation in the Yangjiaping section, Hunan Province (Macouin et al., 2004). Although there are some uncertainties related to stratigraphic correlation between the two sections, the cap carbonate at the base of the Doushantuo Formation and the Doushantuo/Dengying boundary are very likely correlatable (Jiang et al., 2011; Zhu et al., 2013b). Samples from the Yangjiaping section were from strata between the cap carbonate and the Doushantuo/Dengying boundary (Fig. 2 in Macouin et al., 2004), mainly covering the upper part of the Doushantuo Formation with another site (S2) in the lower part of the Doushantuo Formation, which was included in the average data (Table 2 in Macouin et al., 2004). Our sampling segment may be correlated to the strata covered by their site S6 or slightly lower, if the $\delta^{13}C$ excursion can be correlated across the platform faces of the Doushantuo basin (Zhu et al., 2007, 2013b; Jiang et al., 2011). The fact that there is no similarity between the two paleomagnetic results suggests that one of the studies (or both) failed to retrieve the primary remanent magnetization.

We suggest that the HC preserved in Member 3 of the Doushantuo Formation in the Yangtze Gorges area (this study) is the primary remanence because (1) the remanence passed a reversal test; (2) its corresponding pole does not resemble any younger paleomagnetic poles reported from the SCB; and (3) the paleolatitude derived from this remanence reasonably fits between the paleolatitudes of latest Cryogenian (the Nantuo Formation; ≤635 Ma) and early Cambrian (Lin et al., 1985). The results from the Yangjiaping section failed to meet these criteria, although they passed a fold test. Because the fold was formed in Jurassic time (HNBGMR, 1988; Macouin et al., 2004), the fold test could not exclude the possibility of a pre-Jurassic remagnetization. In fact, the paleomagnetic pole from the Yangjiaping section (Macouin et al., 2004) resembles the Early Cambrian (Lin et al., 1985) and Silurian poles (Opdyke et al., 1987; Huang et al., 2000) of the SCB and conflicts with the numerous Ediacaran geomagnetic reversals observed from stratigraphic successions in Australia (Sohl et al., 1999; Raub, 2008; Schmidt et al., 2009; Schmidt and Williams, 2010). Thus, it is likely that the paleomagnetic results from the Yangjiaping section record an early Paleozoic remagnetization.

4. Paleogeographic implications

4.1. Late Neoproterozoic paleolatitudinal changes of SCB

Our new results, in combination with previously published high-quality Neoproterozoic paleomagnetic data (Table 2), depict notable paleolatitudinal changes of the SCB from ca. 800 Ma to ca. 530 Ma (Fig. 7b). In the Yangtze Gorges area, the upper part of the Liantuo Formation is recently considered younger (e.g., ~720 Ma, in Li et al., 2013) than previously thought (748 ± 12 Ma, Ma et al., 1984), because some younger detrital zircon grains are found from this formation and correlative strata, using SHRIMP or ICP-MS methods (Gao et al., 2011; Du et al., 2013; Liu et al., 2013), although neither may conclusively determine the depositional age of this formation. An unresolved question is why the Liantuo paleomagnetic pole (ca. 720 Ma; Evans et al., 2000) resembles the Nantuo pole (ca. 636 Ma; Zhang et al., 2013), both of which passed

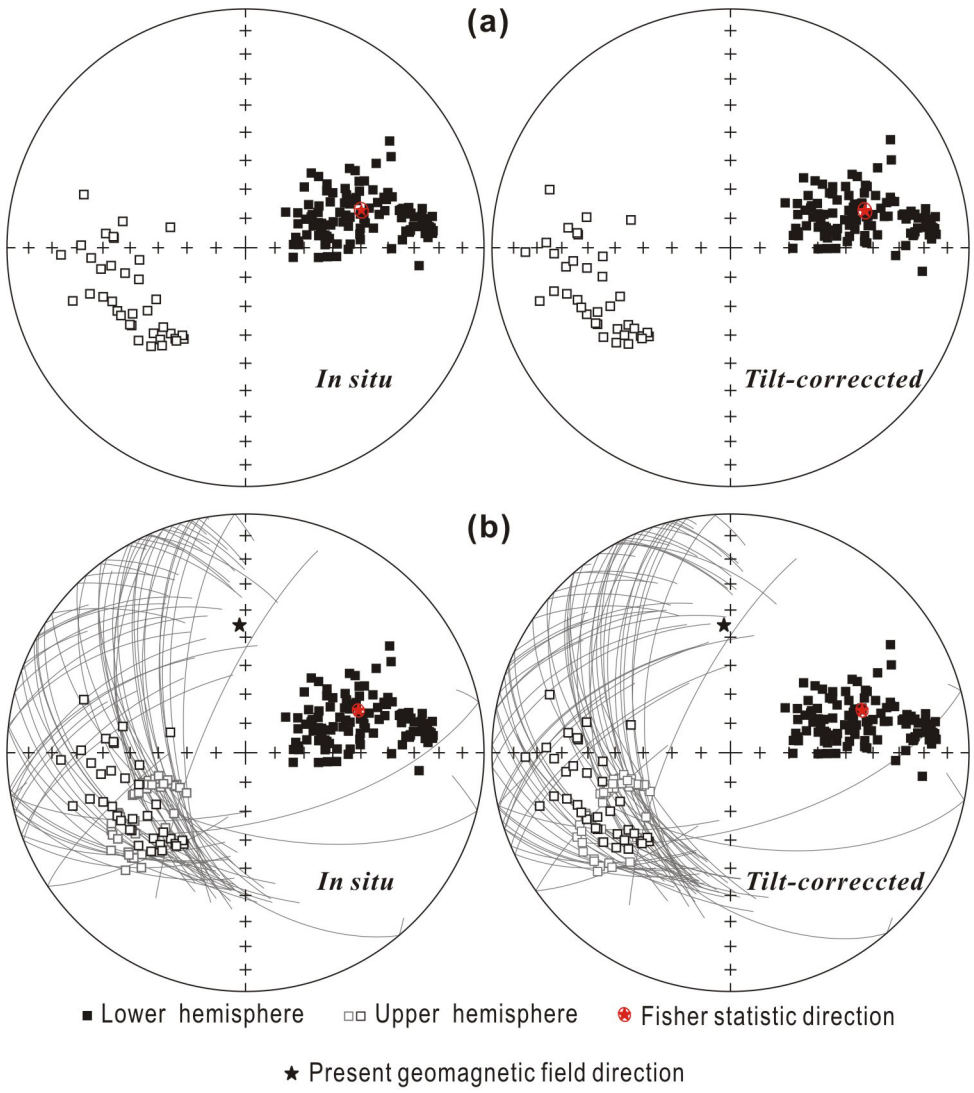

Fig. 6. Equal area projections of the high-temperature component directions. (a) Components are all vectors, identified using principal component analysis. (b) Components combining all vectors and arc constraints.

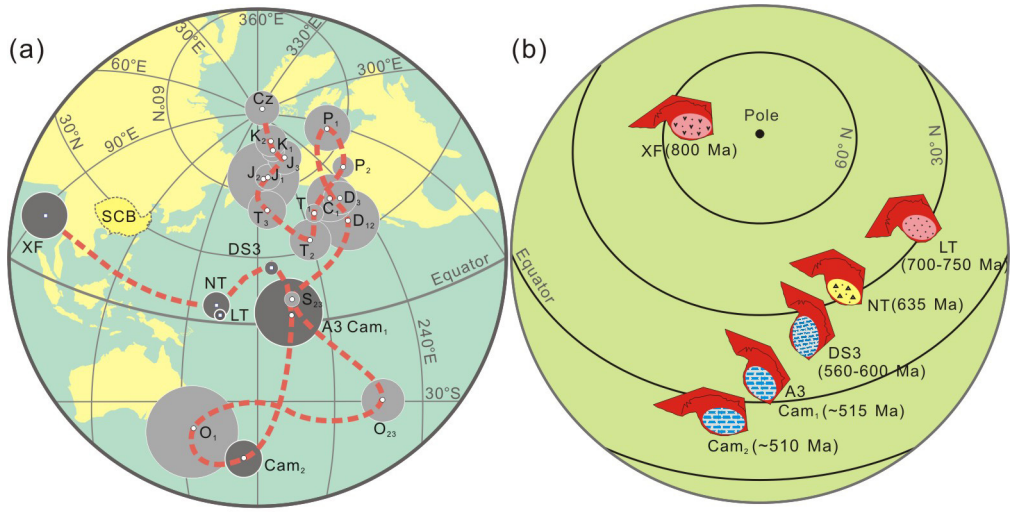

Fig. 7. (a) Apparent polar wander path (APWP) of the SCB since ~800 Ma; the Precambrian and Cambrian poles are colored dark gray and younger poles are light gray. All poles are listed in Table 2. (b) Paleolatitude and orientation variations of the SCB between ~800 Ma and Middle Cambrian based on the paleomagnetic poles in Table 2. Longitude for each paleogeographic position is arbitrary. Patterns represent major geological features for each stage: ca. 800 Ma: bimodal volcanic rocks and red beds; ca. 750–700 Ma: red beds; ca. 635 Ma: Marinoan glacial deposits; ca. 600–560 Ma: carbonates with acanthomorphs and prominent negative $\delta^{13}C$ excursion; ca. 515 Ma–510 Ma: phosphorite-bearing black shale and limestone. Absolute ages assigned for Cambrian poles are based on the stratigraphic correlation of Zhu (2010).

Table 2
Paleomagnetic poles selected for APWPs and reconstructions in Figs. 7–9.

Age (Ma)	Pole	Rock unit	Plat (° N)	Plong (° E)	A_{95} (dm/dp) (°)	Notes and References
Australia						
~505	HR/JC	Middle Cambrian	19.3	219.1	10	Mitchell et al. (2010)
~520	Todd	Todd river dolomite, Allua Fm, Eninta Fm	43.2	159.9	5.9	Kirschvink (1978)
~540	A2[a]	Early Cambrian	37.0	160.8	6.7	McElhinny et al. (2003)
~550	ARL	Arumbera sandstone, N Australia	53.9	168.1	8.8	Mitchell et al. (2010)
~550	AEC	Arumbera sandstone	59.9	144.3	12.7	Mitchell et al. (2010)
~550	IAR	L Arumbera Fm, U Pertatataka Fm	44.3	161.9	10.2	Grey and Corkeron (1998), Kirschvink (1978)
~550	A1[a]	Average above 3 for ~550 Ma	53.1	159.1	16.2	
~560	Wo	Wonoka Fm, S Australia	5.2	210.5	6.8/3.6	Schmidt and Williams (2010)
~580	By	Bunyeroo Fm, S Australia	18.1	196.3	11.8/6.5	Schmidt and Williams (2010)
~590	Br	Brachina Fm, S Australia	46	135.4	4.6/2.4	Schmidt et al. (2009)
~635	NU	Nuccaleena Fm, S Australia	32.3	170.8	3.9/2.2	Schmidt et al. (2009)
~635	EF	Elatina Fm, S Australia	43.7	179.3	4.2/2.1	Schmidt et al. (2009), Sohl et al. (1999)
>635	YA	Yaltipena Fm, S Australia	44.2	172.7	11.4/5.9	Sohl et al. (1999)
India						
~560–635	Marwar	Jodhpur Fm	−1.0	344.0	9.0/5.0	Davis et al. (2013)
South China Block (SCB)						
	Cz[a]	Cenozoic	87.5	315.6	5.9	Huang et al. (2008)
	K_2[a]	Late Cretaceous	75.5	205.3	4.5	Huang et al. (2008)
	K_1[a]	Early Cretaceous	79.0	208.3	5.9	Huang et al. (2008)
	J_3[a]	Late Jurassic	71.0	215.1	6.7	Huang et al. (2008)
	J_2[a]	Middle Jurassic	65.0	186.2	15.0	Enkin et al. (1992)
	J_1[a]	Early Jurassic	65.5	190.9	5.3	Zhao et al. (1996)
	T_3[a]	Late Triassic	51.4	187.2	8.5	Wu et al. (1998)
	T_2[a]	Middle Triassic	34.7	209.4	9.1	Huang et al. (2008)
	T_1[a]	Early Triassic	45.0	216.8	3.9	Huang et al. (2008)
	P_2[a]	Late Permian	53.4	247.7	4.0	Huang et al. (2008)
	P_1	Early Permian	65.3	265.2	8.1/4.2	Wu et al. (1998)
	C_1	Early Carboniferous	47.5	229.1	9.6/4.8	Zhang et al. (2001)
	D_3	Late Devonian	45.4	234.1	6.6/3.3	Zhang et al. (2001)
	D_{12}	Early and Middle Devonian	36.1	231.4	12.5/6.5	Zhang et al. (2001)
	S_{23}[a]	Middle and Late Silurian	10.3	195.8	3.3	Opdyke et al. (1987), Huang et al. (2000)
	O_{23}	Middle and Late Ordovician	−29.5	227.1	6.3	Zhang et al. (2012a)
	O_1	Early Ordovician	−38.4	154.9	14.2/7.4	Wu et al. (1998)
~510[b]	Cam_2[a]	Middle Cambrian	−47.6	174.5	5.2	Bai et al. (1998), Yang et al. (2004)
~515[b]	A3[a]	Early Cambrian, Tianheban & Hetang Fms	5.3	192.7	15.0	Lin et al. (1985)
~560–600	DS3	Member 3 of Doushantuo Fm	23.9	187.0	3.0/1.8	This study
636 ± 5	NT	Nantuo Fm	7.5	161.6	5.9	Zhang et al. (2013)
748 ± 12	LT	Liantuo Fm, CIT subset	3.4	163.6	2.7/2.1	Evans et al. (2000)
802 ± 10	XF	Xiaofeng dykes	13.5	91	11.3/10.5	Li et al. (2004)
Tarim						
~615	Zm	Zhamoketi Fm	−4.9	146.7	3.0	Zhao et al. (2014)
635–615	Sb	Sugetbrak Fm	19.1	149.7	9.3	Zhan et al. (2007)
~635	Tr	Tereeken Fm	27.6	140.4	8.8	Zhao et al. (2014)

Fm, Formation; Plat/Plon, latitude/longitude of VGP; A_{95}, radius of circle with 95% confidence about the palaeopole. Other abbreviations are the same as in Table 1.
[a] Averaging poles.
[b] Absolute age is assigned based on the stratigraphic correlation by Zhu (2010).

magnetostratigraphic field stability tests. Possible interpretations may include that (1) the Liantuo Formation is not much older than the Nantuo Formation in the Yangtze Gorges area, (2) the SCB did not have much paleolatitudinal/orientational change during the Cryogenian, or (3) significant Cryogenian paleolatitudinal/orientational changes of SCB have not been discovered yet.

In spite of this uncertainty, available paleomagnetic data clearly demonstrate that the SCB was located at high latitudes (≥60° N) at ca. 800 Ma and then moved toward mid-latitudes (≥30° N) by ca. 700 or 750 Ma. The drifting path of the SCB from ca. 800 Ma to ca. 750 Ma is less certain, but if the continental block did not have significant rotation, it may have passed through the polar region. Intensive magmatic activity occurred in the SCB when it was in the high-latitude location, which has been interpreted as resulting from an upwelling mantle plume associated with the breakup of the supercontinent Rodinia (Li et al., 2003) or from a long-lived active continental margin of Rodinia (Cawood et al., 2013). The high-latitudinal pre-Cryogenian sedimentary rocks, up to a few thousand meters thick, are predominately reddish clastic sandstone, siltstone and shales, suggesting a likely greenhouse climate condition before the Cryogenian Period. The SCB was located at mid-latitudes during the Cryogenian glaciations (Sturtian and Marinoan) and then moved slowly southward toward the paleoequator during Ediacaran and early Cambrian time (ca. 635–510 Ma, Fig. 7b).

Determination of the geomagnetic field polarity in Precambrian time may be aided from the information of independent evidence, such as paleocurrent or trade-wind directions (Zhang et al., 2012b). But in most cases, polarity is determined on the basis of the coherence of paleocontinental drift rate interpreted from the paleomagnetic data available. The SCB is placed in the northern hemisphere during the late Neoproterozoic and early Cambrian because its northern hemisphere positions minimize the Proterozoic–Phanerozoic apparent polar wander path of the SCB (Fig. 7a). It is also consistent with the use of the Laurentian database in the global reconstruction during the late Neoproterozoic (Li et al., 2013). According to this analysis, we can conclude that the east and down HC polarity of the upper part of Doushantuo Member 3 is geomagnetically Normal, and its antipodal HC direction is Reverse (Fig. 2).

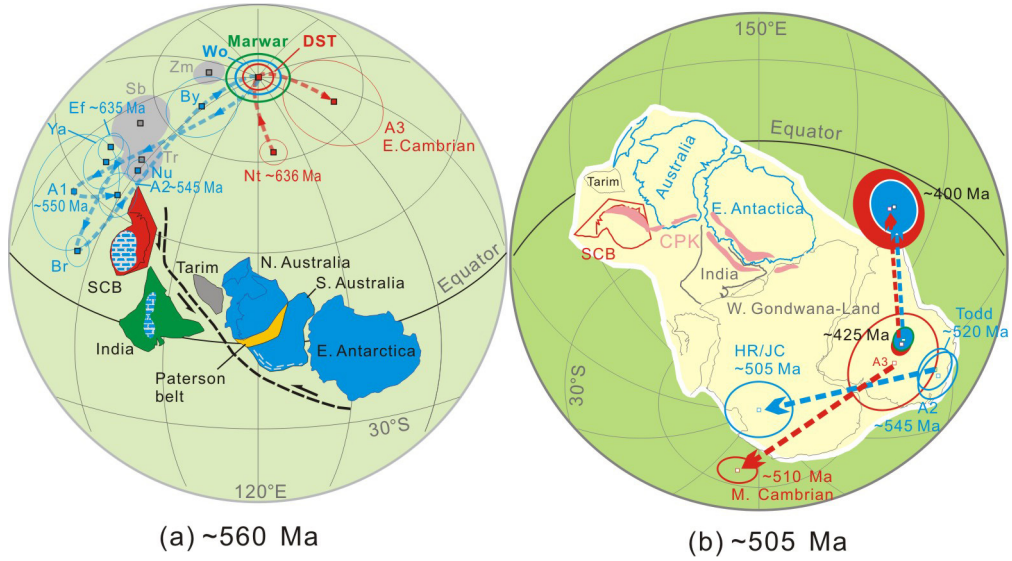

Fig. 8. (a) APWP fit and paleogeographic reconstruction of the SCB, India, Australian blocks, East Antarctica and Tarim at ca. 570–560 Ma, based on the Doushantuo Member 3-Wonoka-Marwar correlation supported by bio- and chemostratigraphy calibrated by U–Pb ages ("option (I)" referred in text). All poles used are listed in Table 2, blocks corresponding to their poles by color. In this snapshot map of ca. 570–560 Ma, paleolatitudes were determined by using the pole of Wonoka Formation for Australian blocks, East Antarctic and Tarim, the pole of the Member 3 of the Doushantuo Formation for the SCB, the pole of the Marwar supergroup for India. Relative cratonic reconstructions were constrained by APWP fit. Euler rotation (47.3, 154.3, 86.4) was used to rotate the Tarim to the southern Australia frame; this link was based on matching three Ediacaran poles of Tarim (Table 2) to the Australian APWP. East Antarctica rotated to southern Australia using (−1.6, 39.0, 31.3) based on those blocks' connection in Gondwana (Powell and Li, 1994). Northern Australia was rotated using Euler rotation (−20, 135, −20) for correcting possible convergence of the Paterson-Petermann orogen according to Li and Evans (2011). Pattern fill on the SCB and India show the proximity of the Ediacaran basins (see text for details). (b) SCB-Gondwana connection in Paleozoic based on an APWP fit after Zhang (2004); the SCB rotated to Australia using (11.3, 148.3, 62.1), Tarim rotated to Australia following that in (a). The paleogeographic reconstruction of Gondwana at ca. 505 Ma used the pole HR/JC from Australia (Mitchell et al., 2010; Table 2). CPK shows a possible link between the Cathaysian Caledonian orogen in the SCB, and the Pinjarra-Prince Charles/Kuungan orogen.

4.2. Ediacaran paleogeographic reconstruction of SCB

Ediacaran apparent polar wander paths (APWPs) of the major continents including Laurentia, Baltica and Australia, show very complex pattern, leading to the hypothesis of true polar wander (Evans, 2003), equatorial dipole geomagnetic field (Abrajevitch and Van der Voo, 2010), rapid plate drifting or complex rotation (Schmidt and Williams, 2010; McCausland et al., 2011; Meert, 2014). The available paleomagnetic data from SCB, however, show no similarity with those APWPs from Laurentia, Baltica and Australia (Fig. 7), indicating that either the SCB was isolated from them, or that substantial Ediacaran apparent polar wander may not yet have been discovered for the SCB.

There has been persistent debate about the paleogeographic relationship between SCB, India and Australia in late Neoproterozoic time (Li et al., 2013; Zhang et al., 2013; Yao et al., 2014; and references therein). Existing reconstructions place the SCB either close to northern India (e.g., Jiang et al., 2003; Zhang et al., 2013; Yao et al., 2014), adjacent to the western side of Australia (e.g., Zhang and Piper, 1997; Yang et al., 2004), or as an isolated continent block close to but not connected with either India or Australia (e.g., Zhou et al., 2002). Our new paleomagnetic results provide some constraints for the possible locations of the SCB during the Ediacaran, but the lack of a direct/reliable age from the sampled stratigraphic interval allows for three alternative reconstruction interpretations as described below.

The samples for our new paleomagnetic data were collected from the uppermost Member 3 of the Doushantuo Formation, about 10 m below a well-dated ash bed of 551.1 ± 0.7 Ma (Condon et al., 2005). Considering that the Doushantuo Formation (ca. 635–551 Ma) covers ~90% of Ediacaran time, a simple age extrapolation would place the sampled interval at ca. 560–570 Ma (e.g., Jiang et al., 2007). This is consistent with the Pb–Pb age of 574 ± 14 Ma from the upper phosphorite layers of the Doushantuo Formation in Weng'an (Chen et al., 2004) and the similarity of acritarch fossils between Jiulongwan and Weng'an sections (e.g., Zhou et al., 2007; Xiao et al., 2014). The Doushantuo Members 3 and 4 host a prominent negative $\delta^{13}C$ excursion that has been correlated with the Shuram $\delta^{13}C$ excursion in Oman (Fike et al., 2006; Le Guerroue, 2010), the Wonoka $\delta^{13}C$ excursion in Australia (Calver, 2000), and the Krol B $\delta^{13}C$ excursion in India (Kaufman et al., 2006; Jiang et al., 2007). The presence of similar acritarchs in Member 2 and lower Member 3 of the Doushantuo Formation and in the Bunyeroo Formation below the Wonoka $\delta^{13}C$ anomaly (Zhou et al., 2007; Liu et al., 2013) and Sr isotope values (Sawaki et al., 2010; Le Guerroue, 2010) support the Doushantuo Member 3–Wonoka Formation correlation. In this case, the combination of the Doushantuo Member 3 paleomagnetic pole (this study), the Wonoka pole (Schmidt and Williams, 2010), and the recently published pole from the Marwar Supergroup (Sonia sandstone, Jodhpur Group) in NW India (ca. 635–560 Ma; Davis et al., 2013) would place the SCB close to northwestern India (Fig. 8a). This position, which we refer to as reconstruction option (I), is broadly consistent with the reconstruction proposed by Jiang et al. (2003) based on the sequence stratigraphic analysis and the tectonic models recently proposed by Yao et al. (2014). Although the paleolongitude can be arbitrary, moving the SCB toward the Australian blocks will not improve the fitting of the APWPs and is thus unnecessary. This reconstruction suggests that the SCB-Australia connection was formed later, during the Ediacaran–Cambrian transition (Zhang, 2004; Zhang et al., 2013), via large-scale sinistral transform motion between SCB + India and Tarim + Australia + East Antarctica (Fig. 8). If this was the case, the Caledonian orogen of the Cathaysia block might be the result of final amalgamation of the East Gondwana ("CPK" depicted in Fig. 8b).

The recently published Re–Os age of 591 ± 5.3 Ma (Zhu et al., 2013a) from the basal Doushantuo Member 4, however, questions

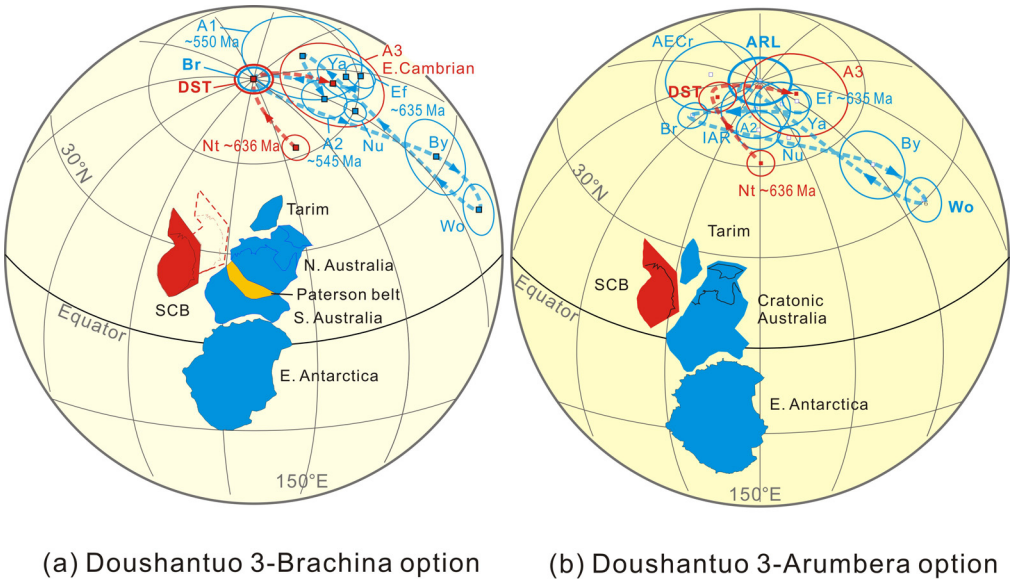

(a) Doushantuo 3-Brachina option (b) Doushantuo 3-Arumbera option

Fig. 9. Alternative paleogeographic reconstructions show the SCB's relations in Ediacaran time. (a) APWP comparisons and possible geographic relations of the SCB if the Re–Os age of 591 ± 5.3 Ma from the basal Member 4 of the Doushantuo Formation is used and a Doushantuo Member 3–Brachina correlation (at ~590–600 Ma, "option (II)" referred in text) is assumed. The dashed outline of the SCB shows its relative position attached to the Australia in Paleozoic depicted in Fig. 8b. (b) APWP comparisons and possible geographic relations of the SCB (at ~550 Ma, "option (III)" referred in text) if assumed the Doushantuo Member 3 is slightly younger than the sampled strata of Wonoka Formation (Schmidt and Williams, 2010) and the Australian APWP jumps back toward the Arumbera Sandstone poles (listed in Table 2). Other symbols are the same as in Fig. 8.

the age assignment of ca. 560 Ma for the sampled interval and the age of the Member 3–4 $\delta^{13}C$ excursion. If we take this Re–Os age as the constraint, then the Doushantuo Member 3 paleomagnetic pole would be better compared with the Brachina pole in Australia and permissibly, the Marwar pole in India. The allowable reconstruction according to this option (II) would place the SCB close to Australia (Fig. 9a), similar to its position attached to NW Australia in Early Paleozoic (Fig. 8b; Zhang, 2004; Zhang et al., 2013). In this case, it implies that the SCB reached a position closed to NW Australia during ca. 600–590 Ma, and that prior to ca. 600 Ma, the SCB was more distant from Australia during and before the Marinoan glaciation. This reconstruction is also consistent with our previous paleomagnetic data for an early Cambrian SCB-Australia connection (Zhang et al., 2013) and with the recent tectonic model of Yao et al. (2014), in which the SCB was considered as an isolated block during the Cryogenian. The reconstruction of option (II) would also be broadly permissible if Doushantuo Member 3 correlates to slightly younger than the Wonoka Formation in Australia, ca. 555 Ma (Option III, Fig. 9b), in which case the joint SCB + Australia APWP has swung back toward the Ediacaran–Cambrian boundary poles of Pertatataka and lower Arumbera Sandstone from central Australia (Kirschvink, 1978).

We favor either of the two younger age options for Doushantuo Member 3. The Re–Os age of 591 ± 5.3 Ma is obtained from a subset of four data points after excluding the other three discordant data points (Zhu et al., 2013a). If all the seven data points are included, an age of 595 ± 22 Ma has enough room to accommodate a direct Doushantuo Member 3–Wonoka correlation, which is supported by existing carbon and strontium isotope chemostratigraphy and biostratigraphy. Such a direct correlation would favor reconstruction option (I). The origin of the Shuram-Wonoka $\delta^{13}C$ excursion has been debated (e.g., Knauth and Kennedy, 2009; Derry, 2010; Schrag et al., 2013), and if the isotopic anomalies are slightly diachronous in the ca. 570–555 Ma range between SCB and Australia, then reconstruction option (III) becomes viable.

The plentiful Ediacaran fossils in the SCB have a salient characteristic. The earliest Ediacaran acanthomorphic acritarch assemblage (the lower *Tianzhushania spinosa* assemblage; Liu et al., 2013) that possibly reflects the rise of the complex animal life, has not been discovered from other continents except for the likely presence in Lesser Himalaya of northern India (Tiwari and Knoll, 1994; Mathur et al., 2009, 2014). Our ~560–570 Ma reconstruction permits the paleogeographic proximity of SCB and northern India during the early Ediacaran Period (Jiang et al., 2003). The preservation of early Ediacaran metazoan fossils in the SCB and northern India implies either a unique paleo-environmental control on permineralization of fossils or the origin and early diversification of post-Marinoan animal life in an isolated, moderate latitudinal corner of the northern hemisphere.

5. Conclusion

A new paleomagnetic pole from the upper Member 3 of the Ediacaran Doushantuo Formation was obtained from the Jiulongwan section in the Yangtze Gorges area, Hubei Province, South China. This paleomagnetic pole represents the first Ediacaran pole in South China that passes a reversal test, and fills the paleomagnetic data gap between poles from the Cryogenian Nantuo Formation and the Early Cambrian. The new pole differs from the previously published Doushantuo paleomagnetic result of the Yangjiaping section, northern Hunan province, which we suggest has been remagnetized during the early Paleozoic. Although there is no direct age constraint for the paleomagnetic pole, existing chemo- and biostratigraphy allows for the Doushantuo Member 3 to correlate either directly with the Australian Wonoka Formation, or perhaps slightly younger Australian units. Depending on these correlations, various tectonic scenarios of paleogeographic evolution during East Gondwana assembly can be envisaged. South China was most likely an isolated continental block located close to northern India during the Ediacaran but was progressively approaching northwestern Australia during the latest Ediacaran and Early Cambrian.

Acknowledgements

Authors greatly appreciate the constructive comments and suggestions from reviewers Natalia Levashova and Rob Van der Voo, and editor Sergei Pisarevsky. This work was jointly

supported by 973 program (2011CB808800), NSFC Projects 40974035, 40032010B and 40572019.

References

Abrajevitch, A., Van der Voo, R., 2010. Incompatible Ediacaran paleomagnetic directions suggest an equatorial geomagnetic dipole hypothesis. Earth Planet. Sci. Lett. 293, 164–170.

Bai, L.X., Zhu, R.X., Wu, H.N., Guo, B., Lü, J.J., 1998. New Cambrian paleomagnetic pole for Yangtze Block. Sci. China Ser. D: Earth Sci. 41, 66–71.

Calver, C.R., 2000. Isotope stratigraphy of the Ediacarian (Neoproterozoic III) of the Adelaide rift complex, Australia, and the overprint of water column stratification. Precambrian Res. 100, 121–150.

Cawood, P.A., Wang, Y.J., Xu, Y.J., Zhao, G.C., 2013. Locating South China in Rodinia and Gondwana: a fragment of greater India lithosphere? Geology 41 (8), 903–906.

Chen, D., Dong, W., Zhu, B., Chen, X.P., 2004. Pb–Pb ages of Neoproterozoic Doushantuo phosphorites in South China: constraints on early metazoan evolution and glaciation events. Precambrian Res. 132, 123–132.

Condon, D., Zhu, M., Bowring, S., Wang, W., Yang, A., Jin, Y., 2005. U–Pb ages from the Neoproterozoic Doushantuo Formation, China. Science 308 (5718), 95–98.

Davis, J.K., Meert, J.G., Pandit, M.K., 2013. Paleomagnetic analysis of the Marwar Supergroup, Rajasthan, India and proposed interbasinal correlations. J. Asian Earth Sci., http://dx.doi.org/10.1016/j.jseaes.2013.09.027.

Derry, L.A., 2010. A burial diagenesis origin for the Ediacaran Shuram-Wonoka carbon isotope anomaly. Earth Planet. Sci. Lett. 294, 152–162.

Dong, J., Zhang, S., Jiang, G., Li, H., Gao, R., 2013. Greigite from carbonate concretions of the Ediacaran Doushantuo Formation in South China and its environmental implications. Precambrian Res. 225, 77–85.

Du, Q., Wang, Z., Wang, J., Qiu, Y., Jiang, X., Deng, Q., Yang, F., 2013. Geochronology and paleoenvironment of the pre-Sturtian glacial strata: evidence from the Liantuo Formation in the Nanhua rift basin of the Yangtze Block, South China. Precambrian Res. 233, 118–131.

Enkin, R.J., Yang, Z., Chen, Y., Courtillot, V., 1992. Paleomagnetic constraints on the geodynamic history of the major blocks of China from the Permian to the present. J. Geophys. Res.: Solid Earth 97, 13953–13989.

Evans, D.A.D., 2003. True polar wander and supercontinents. Tectonophysics 362, 303–320.

Evans, D.A.D., Li, Z.X., Kirschvink, J.L., Wingate, M.T.D., 2000. A high-quality mid-Neoproterozoic paleomagnetic pole from South China, with implications for ice ages and the breakup configuration of Rodinia. Precambrian Res. 100 (1–3), 313–334.

Fike, D.A., Grotzinger, J.P., Pratt, L.M., Summons, R.E., 2006. Oxidation of the Ediacaran Ocean. Nature 444, 744–747.

Gao, S., Yang, J., Zhou, L., Li, M., Hu, Z., Guo, J., Yuan, H., Gong, H., Xiao, G., Wei, J., 2011. Age and growth of the Archean Kongling terrain, South China, with emphasis on 3.3 Ga granitoid gneisses. Am. J. Sci. 311 (2), 153–182.

Grey, K., Corkeron, M., 1998. Late Neoproterozoic stromatolites in glacigenic successions of the Kimberley region, Western Australia: evidence for a younger Marinoan glaciation. Precambrian Res. 92 (1), 65–87.

Haggart, J.W., Ward, P.D., Raub, T.D., Carter, E.S., Kirschvink, J.L., 2009. Molluscan biostratigraphy and paleomagnetism of Campanian strata, Queen Charlotte Islands, British Columbia: implications for Pacific coast North America biochronology. Cretaceous Res. 30 (4), 939–951.

Hoffman, P.F., Li, Z.-X., 2009. A palaeogeographic context for Neoproterozoic glaciation. Palaeogeogr. Palaeoclimatol. Palaeoecol. 277 (3–4), 158–172.

HNBGMR (Hunan Bureau of Geology and Mineral Resources), 1988. Regional geology of Hunan Province. People's Republic of China Ministry of Geology and Mineral Resources Geological Memoirs, 8, Geological Publishing House, Beijing, pp. 698pp.

Huang, B.C., Zhou, Y.X., Zhu, R.X., 2008. Discussions on Phanerozoic evolution and formation of continental China, based on paleomagnetic studies. Earth Sci. Front. 15, 348–359.

Huang, K., Opdyke, N.D., Zhu, R.X., 2000. Further paleomagnetic results from the Silurian of the Yangtze Block and their implications. Earth Planet. Sci. Lett. 175, 191–202.

Jiang, G., Kaufman, A.J., Christie-Blick, N., Zhang, S., Wu, H., 2007. Carbon isotope variability across the Ediacaran Yangtze platform in South China: implications for a large surface-to-deep ocean delta C-13 gradient. Earth Planet. Sci. Lett. 261, 303–320.

Jiang, G., Shi, X., Zhang, S., Wang, Y., Xiao, S., 2011. Stratigraphy and paleogeography of the Ediacaran Doushantuo Formation (ca. 635–551 Ma) in South China. Gondwana Res. 19 (4), 831–849.

Jiang, G., Sohl, L.E., Christie-Blick, N., 2003. Neoproterozoic stratigraphic comparison of the Lesser Himalaya (India) and Yangtze block (South China): paleogeographic implications. Geology 31 (10), 917–920.

Kaufman, A.J., Jiang, G., Christie-Blick, N., Banerjee, D.M., Rai, V., 2006. Stable isotope record of the terminal Neoproterozoic Krol platform in the Lesser Himalayas of northern India. Precambrian Res. 147, 156–185.

Kirschvink, J.L., 1978. The Precambrian–Cambrian boundary problem: paleomagnetic directions from the Amadeus Basin, Central Australia. Earth Planet. Sci. Lett. 40 (1), 91–100.

Kirschvink, J.L., 1980. The least-squares line and plane and the analysis of palaeomagnetic data. Geophys. J. Royal Astronom. Soc. 62 (3), 699–718.

Kirschvink, J.L., Kopp, R.E., Raub, T.D., Baumgartner, C.T., Holt, J.W., 2008. Rapid, precise, and high-sensitivity acquisition of paleomagnetic and rock-magnetic data: development of a low-noise automatic sample changing system for superconducting rock magnetometers. Geochem. Geophys. Geosyst. 9 (5), Q05Y01.

Knauth, L.P., Kennedy, M.J., 2009. The late Precambrian greening of the Earth. Nature 460, 728–732.

Le Guerroue, E., 2010. Duration and synchroneity of the largest negative carbon isotope excursion on Earth: the Shuram/Wonoka anomaly. C. R. Geosci. 342, 204–214.

Li, W.-X., Li, X.-H., Li, Z.-X., Lou, F.-S., 2008. Obduction-type granites within the NE Jiangxi Ophiolite: implications for the final amalgamation between the Yangtze and Cathaysia Blocks. Gondwana Res. 13 (3), 288–301.

Li, X.-H., Li, Z.-X., Li, W.-X., 2014. Detrital zircon U–Pb age and Hf isotope constrains on the generation and reworking of Precambrian continental crust in the Cathaysia Block, South China: a synthesis. Gondwana Res. 25, 1202–1215.

Li, Z.X., Li, X.H., Kinny, P.D., Wang, J., Zhang, S., Zhou, H.W., 2003. Geochronology of Neoproterozoic syn-rift magmatism in the Yangtze Craton, South China and correlations with other continents: evidence for a mantle superplume that broke up Rodinia. Precambrian Res. 122 (1–4), 85–109.

Li, Z.-X., Evans, D.A.D., 2011. Late Neoproterozoic 40° intraplate rotation within Australia allows for a tighter-fitting and longer-lasting Rodinia. Geology 39 (1), 39–42.

Li, Z.-X., Evans, D.A.D., Halverson, G.P., 2013. Neoproterozoic glaciations in a revised global palaeogeography from the breakup of Rodinia to the assembly of Gondwanaland. Sediment. Geol. 294, 219–232.

Li, Z.X., Evans, D.A.D., Zhang, S., 2004. A 90° spin on Rodinia: possible causal links between the Neoproterozoic supercontinent, superplume, true polar wander and low-latitude glaciation. Earth Planet. Sci. Lett. 220, 409–421.

Lin, J.L., Fuller, M., Zhang, W.Y., 1985. Paleogeography of the north and south China blocks during the Cambrian. J. Geodyn. 2, 91–114.

Liu, P., Yin, C., Gao, L., Tang, F., Chen, S., 2009. New material of microfossils from the Ediacaran Doushantuo Formation in the Zhangcunping area, Yichang, Hubei Province and its zircon SHRIMP U–Pb age. Chin. Sci. Bull. 54, 1058–1064.

Liu, P., Yin, C., Chen, S., Tang, F., Gao, L., 2013. The biostratigraphic succession of acanthomorphic acritarchs of the Ediacaran Doushantuo Formation in the Yangtze Gorges area, South China and its biostratigraphic correlation with Australia. Precambrian Res. 225, 29–43.

Liu, X., Nie, Y., Sun, L., Emslie, S.D., 2013. Eco-environmental implications of elemental and carbon isotope distributions in ornithogenic sediments from the Ross Sea region, Antarctica. Geochim. Cosmochim. Acta 117, 99–114.

Lowrie, W., 1990. Identification of ferromagnetic minerals in a rock by coercivity and unblocking temperature properties. Geophys. Res. Lett. 17 (2), 159–162.

Ma, G., Li, H., Zhang, Z., 1984. An investigation of the age limits of the Sinian System in South China. Bull. Yichang Inst. Geol. Miner. Resour. 8, 1–29.

Macouin, M., Besse, J., Ader, M., Gilder, S., Yang, Z., Sun, Z., Agrinier, P., 2004. Combined paleomagnetic and isotopic data from the Doushantuo carbonates, South China: implications for the "snowball Earth" hypothesis. Earth Planet. Sci. Lett. 224 (3–4), 387–398.

Mathur, V.K., Mishra, V.P., Nath, S., 2009. Discovery of animal eggs and embryos from the Ediacaran (Terminal Proterozoic) Chambaghat Formation, Krol Group, Himachal Lesser Himalaya. J. Geol. Soc. India 74, 498–502.

Mathur, V.K., Shome, S., Nath, S., Babu, R., 2014. First record of metazoan eggs and embryos from early Cambrian Chert Member of Deo ka Tibba Formation, Tal Group, Uttarakhand Lesser Himalaya. J. Geol. Soc. India 83, 191–197.

McCausland, P.J.A., Hankard, F., Van der Voo, R., Hall, C.M., 2011. Ediacaran paleogeography of Laurentia: paleomagnetism and ^{40}Ar–^{39}Ar geochronology of the 583 Ma Baie des Moutons syenite, Quebec. Precambrian Res. 187, 58–78.

McElhinny, M.W., Powell, C.M., Pisarevsky, S.A., 2003. Paleozoic terranes of eastern Australia and the drift history of Gondwana. Tectonophysics 362 (1–4), 41–65.

McFadden, P.L., McElhinny, M.W., 1988. The combined analysis of remagnetization circles and direct observations in palaeomagnetism. Earth Planet. Sci. Lett. 87 (1–2), 161–172.

McFadden, P.L., McElhinny, M.W., 1990. Classification of the reversal test in palaeomagnetism. Geophys. J. Int. 103 (3), 725–729.

Meert, J.G., 2014. Ediacaran – Early Ordovician paleomagnetism of Baltica: a review. Gondwana Res. 25, 159–169.

Mitchell, R.N., Evans, D.A.D., Kilian, T.M., 2010. Rapid Early Cambrian rotation of Gondwana. Geology 38 (8), 755–758.

Opdyke, N.D., Huang, K., Xu, G., Zhang, W.Y., Kent, D.V., 1987. Paleomagnetic results from the Silurian of the Yangtze paraplatform. Tectonophysics 139, 123–132.

Özdemir, Ö., Dunlop, D.J., Moskowitz, B.M., 2002. Changes in remanence, coercivity and domain state at low temperature in magnetite. Earth Planet. Sci. Lett. 194 (3–4), 343–358.

Powell, C., Li, Z., 1994. Reconstruction of the Panthalassan margin of Gondwanaland. Permian–Triassic Pangean basins and foldbelts along the Panthalassan margin of Gondwanaland. Geol. Soc. Am. Memoir 184, 5–9.

Raub, T.D., 2008. Prolonged Deglaciation of Snowball Earth. Ph.D. thesis, Yale University, New Haven.

Sawaki, Y., Ohno, T., Tahata, M., Komiya, T., Hirata, T., Maruyama, S., Windley, B.F., Han, J., Shu, D., Li, Y., 2010. The Ediacaran radiogenic Sr isotope excursion in the Doushantuo Formation in the Three Gorges area, South China. Precambrian Res. 176, 46–64.

Schmidt, P.W., 2014. A review of Precambrian palaeomagnetism of Australia: palaeogeography, supercontinents, glaciations and true polar wander. Gondwana Res. 25, 1164–1185.

Schmidt, P.W., Williams, G.E., 2010. Ediacaran palaeomagnetism and apparent polar wander path for Australia: no large true polar wander. Geophys. J. Int. 182, 711–726.
Schmidt, P.W., Williams, G.E., McWilliams, M.O., 2009. Palaeomagnetism and magnetic anisotropy of late Neoproterozoic strata, South Australia: implications for the palaeolatitude of late Cryogenian glaciation, cap carbonate and the Ediacaran System. Precambrian Res. 174 (1–2), 35–52.
Schrag, D.P., Higgins, J.A., Macdonald, F.A., Johnston, D.T., 2013. Authigenic carbonate and the history of the global carbon cycle. Science 339, 540–543.
Sohl, L.E., Christie-Blick, N., Kent, D.V., 1999. Paleomagnetic polarity reversals in Marinoan (ca. 600 Ma) glacial deposits of Australia: implications for the duration of low-latitude glaciation in Neoproterozoic time. Geol. Soc. Am. Bull. 111 (8), 1120–1139.
Tahata, M., Ueno, Y., Ishikawa, T., Sawaki, Y., Murakami, K., Han, J., Shu, D., Li, Y., Guo, J., Yoshida, N., Komiya, T., 2013. Carbon and oxygen isotope chemostratigraphies of the Yangtze platform, South China: decoding temperature and environmental changes through the Ediacaran. Gondwana Res. 23, 333–353.
Tauxe, L., Kent, D.V., 2004. A simplified statistical model for the geomagnetic field and the detection of shallow bias in paleomagnetic inclinations: was the ancient magnetic field dipolar? Timescales of the Paleomagnetic Field. AGU, Washington, DC, pp. 101–115.
Tiwari, M., Knoll, A.H., 1994. Large acanthomorphic acritarchs from the Infra krol Formation of the Lesser Himalaya and their stratigraphic significance. J. Himalayan Geol. 5, 193–201.
Wu, H.N., Zhu, R.X., Bai, L.X., Guo, B., Lü, J.J., 1998. Revised apparent polar wander path of the Yangtze Block and its tectonic implications. Sci. China Ser. D: Earth Sci. 41, 78–90.
Xiao, S., Zhou, C., Liu, P., Wang, D., Yuan, X., 2014. Phosphatized acanthomorphic acritarchs and related microfossils from the Ediacaran Doushantuo Formation at Weng'an (South China) and their implications for biostratigraphic correlation. J. Paleontol. 88, 1–67.
Yang, Z., Sun, Z., Yang, T., Pei, J., 2004. A long connection (750–380 Ma) between South China and Australia: paleomagnetic constraints. Earth Planet. Sci. Lett. 220, 423–434.
Yao, W.-H., Li, Z.-X., Li, W.-X., Li, X.-H., Yang, J.-H., 2014. From Rodinia to Gondwanaland: a tale of detrital zircon provenance analyses from the southern Nanhua Basin, South China. Am. J. Sci. 314, 278–313.
Zhan, S., Chen, Y., Xu, B., Wang, B., Faure, M., 2007. Late Neoproterozoic paleomagnetic results from the Sugetbrak Formation of the Aksu area, Tarim basin (NW China) and their implications to paleogeographic reconstructions and the snowball Earth hypothesis. Precambrian Res. 154, 143–158.
Zhang, Q.R., Li, X.H., Feng, L.J., Huang, J., Song, B., 2008a. A new age constraint on the onset of the Neoproterozoic glaciations in the Yangtze Platform, South China. J. Geol. 116, 423–429.
Zhang, Q.R., Piper, J.D.A., 1997. Palaeomagnetic study of Neoproterozoic glacial rocks of the Yangzi Block: palaeolatitude and configuration of South China in the late Proterozoic Supercontinent. Precambrian Res. 85 (3–4), 173–199.
Zhang, S., 2004. South China's Gondwana connection in the Paleozoic: paleomagnetic evidence. Progr. Nat. Sci. 14 (1), 85–90.
Zhang, S., Evans, D.A.D., Li, H., Wu, H., Jiang, G., Dong, J., Zhao, Q., Raub, T.D., Yang, T., 2013. Paleomagnetism of the late Cryogenian Nantuo Formation and paleogeographic implications for the South China Block. J. Asian Earth Sci. 72, 164–177.
Zhang, S., Jiang, G., Dong, J., Han, Y., Wu, H., 2008b. New SHRIMP U–Pb age from the Wuqiangxi Formation of Banxi Group: implications for rifting and stratigraphic erosion associated with the early Cryogenian (Sturtian) glaciation in South China. Sci. China Ser. D: Earth Sci. 51 (11), 1537–1544.
Zhang, S., Jiang, G., Han, Y., 2008c. The age of the Nantuo Formation and Nantuo glaciation in South China. Terra Nova 20 (4), 289–294.
Zhang, S., Jiang, G., Zhang, J., Song, B., Kennedy, M.J., Christie-Blick, N., 2005. U–Pb sensitive high-resolution ion microprobe ages from the Doushantuo Formation in South China: constraints on late Neoproterozoic glaciations. Geology 33 (6), 473–476.
Zhang, S., Li, H., Zhang, X., Liu, Y., Cao, Q., 2012a. New Ordovician paleomagnetic results from South China Block and their paleogeographic implications. In: The 34th IGC abstract.
Zhang, S., Li, Z.-X., Evans, D.A.D., Wu, H., Li, H., Dong, J., 2012b. Pre-Rodinia supercontinent Nuna shaping up: a global synthesis with new paleomagnetic results from North China. Earth Planet. Sci. Lett. 353–354, 145–155.
Zhang, S., Zhu, H., Meng, X., 2001. New paleomagnetic results from the Devonian-Carboniferous successions in the Southern Yangtze Block and their paleogeographic implications. Acta Geol. Sin. 75, 303–313.
Zhao, P., Chen, Y., Zhan, S., Xu, B., Faure, M., 2014. The Apparent Polar Wander Path of the Tarim block (NW China) since the Neoproterozoic and its implications for a long-term Tarim–Australia connection. Precambrian Res. 242, 39–57.
Zhao, X., Coe, R.S., Gilder, S.A., Frost, G.M., 1996. Palaeomagnetic constraints on the palaeogeography of China: implications for Gondwanaland. Aust. J. Earth Sci. 43, 643–672.
Zhou, C., Tucker, R., Xiao, S., Peng, Z., Yuan, X., Chen, Z., 2004. New constraints on the ages of Neoproterozoic glaciations in South China. Geology 32 (5), 437–440.
Zhou, C., Xiao, S., 2007. Ediacaran $\delta^{13}C$ chemostratigraphy of South China. Chem. Geol. 237, 89–108.
Zhou, C., Xie, G., McFadden, K., Xiao, S., Yuan, X., 2007. The diversification and extinction of Doushantuo-Pertatataka acritarchs in South China: causes and biostratigraphic significance. Geol. J. 42, 229–262.
Zhou, M.-F., Yan, D.-P., Kennedy, A.K., Li, Y., Ding, J., 2002. SHRIMP U–Pb zircon geochronological and geochemical evidence for Neoproterozoic arc-magmatism along the western margin of the Yangtze Block, South China. Earth Planet. Sci. Lett. 196, 51–67.
Zhu, B., Becker, H., Jiang, S.-Y., Pi, D.-H., Fischer-Goedde, M., Yang, J.-H., 2013a. Re–Os geochronology of black shales from the Neoproterozoic Doushantuo Formation, Yangtze platform, South China. Precambrian Res. 225, 67–76.
Zhu, M., 2010. The origin and Cambrian explosion of animals: fossil evidence from China. Acta Palaeontol. Sin. 49 (3), 269–287.
Zhu, M., Lu, M., Zhang, J., Zhao, F., Li, G., Yang, A., Zhao, X., Zhao, M., 2013b. Carbon isotope chemostratigraphy and sedimentary facies evolution of the Ediacaran Doushantuo Formation in western Hubei, South China. Precambrian Res. 225, 7–28.
Zhu, M., Zhang, J., Yang, A., 2007. Integrated Ediacaran (Sinian) chronostratigraphy of South China. Palaeogeogr. Palaeoclimatol. Palaeoecol. 254, 7–61.